COMPUTATIONAL CHARACTERIZARION OF MICROWAVE-ENHANCED CVI PRODUCTION OF SiCf/SiC COMPOSITES

M.T. Porter[1], J. Binner[1], P. Kumi[2], K.E. Stern[2], V.V. Yakovlev[2]

[1] *School of Metallurgy and Materials, University of Birmingham, Edgbaston, Birmingham, B15 2TT, UK*
[2] *Department of Mathematical Sciences, Worcester Polytechnic Institute, Worcester, MA 01609, USA*
vadim@wpi.edu

Keywords: energy coupling, microwave heating, modelling, SiC composites, temperature field.

1. Introduction

The aerospace industry is one of the largest and arguably the most important to the composite materials sector. For many aerospace applications, the exceptional mechanical properties of composites, such as high strength, low weight and high stiffness are of utmost importance [1]. To this end, they have seen a recent explosion in the industry as manufacturing has become more advanced and cheaper.

Silicon carbide fibre reinforced silicon carbide matrix composites (SiC_f/SiC) have been identified as a material with high-performance mechanical properties [2-7]. The application of SiC_f/SiC in the aerospace industry is increasing; for instance, replacing Ni-Ti super-alloy components and thus giving engines the capability to operate at higher temperatures would lead to reduced active cooling requirement and enhanced thermal efficiency [5].

One advanced manufacturing technique, chemical vapour infiltration (CVI), can create an extremely refined microstructure with little or no preform degradation and minimal residual stresses [9-11]. CVI is the process of infiltrating a porous matrix of typically continuous fibres (a preform) with a mixture of precursor gases that react, decompose, and deposit a solid matrix at high temperature. The primary objective of CVI, like the other advanced manufacturing methods, is to increase the density of the porous preform to as close to 100% of theoretical density as possible [10]. CVI's challenges, however, are three-fold:

(a) Batch production times are typically 2-3 months.
(b) Premature pore closure results in low efficiencies.
(c) Subsequently, associated manufacturing costs are very high.

Microwave-enhanced (ME) CVI heating of ceramic matrix composites has been proposed as a potential solution to these challenges [2, 3, 5]. It produces a favourable "inverse" temperature profile, meaning the temperature is hottest, in contrast to conventional CVI, within the heated sample [2, 3, 5, 7]. This profile initiates densification at the centre of the sample, thus avoiding surface porosity closure. It has also recently been shown that this process has the potential to yield near fully dense SiC_f/SiC composites in a significantly shorter time span [7]. This work demonstrated proof of concept that an "inverse" densification profile could be achieved with the SiC deposit of nearly stochiometric composition and a highly crystalline microstructure.

This paper presents some results of computational analysis of electromagnetic (EM) and thermal characteristics of the ME CVI process carried out with thin (thickness *h* from 8 to 24 mm) SiC discs (diameter *d* from 55 to 165 mm) in a Labotron microwave system from SAIREM. The simulations aimed to clarify multiple unexplained observations in experimental work [7] through understanding causes for the formation of microwave-induced temperature fields. With the use of the developed EM model, resonant and non-
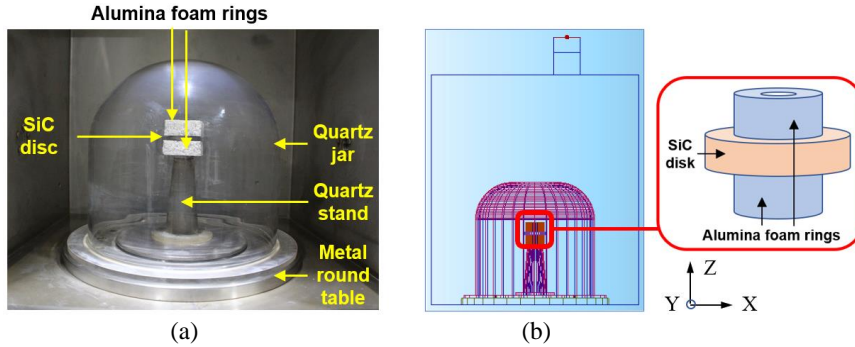
Fig. 1. Photo of the experimental setup in the Labotron HTE M30KLB Pro systems (SAIREM) (a) and a 2D view of the corresponding *QuickWave* model (b).

resonant frequencies of the experimental system for different temperatures of the processed SiC sample were analysed to explain the difference in heating rates. With the EM-thermal coupled model, 3D temperature fields in the SiC preforms at different frequencies were then simulated. It was shown that, while being highly non-uniform in the beginning of the process, temperature patterns evolve to quite homogeneous ones by its end. The results suggest a means for better control of the equipment to pave the way to more efficient implementations of ME CVI the hence the less expensive and high quality SiC_f/SiC composites.

2. Experimental Work

The customised microwave power system (Labotron HTE M30KB CL PRO, SAIREM, France) included a microwave generator, a control unit, and 550 x 550 x 610 mm 316l polished stainless-steel cavity. The 2.45 GHz magnetron-based microwave generator (Muegge GmbH, Germany) had a maximum power output of 3.0 kW that could be adjusted in 10 W increments. The feeding rectangular waveguide was located at the top of the cavity in the back right-hand corner. The microwaves were attenuated by a manual E/H tuner (SAIREM, France) and a four-stub auto tuner (SAIREM, France). Their combined use aimed to minimise the reflected power within the cavity and improve the impedance matching, coupling and subsequent heating of the SiC samples.

The processed SiC preforms were made in a disc form from multiple circular patches cut out from the sheets of SiC fabric (COI Ceramics, Inc., CA, USA) that were stitched by a cotton thread. Most of the experiments were done with the discs of $d = 55$ m and $h = 8$ mm and contents of air up to 20 %. Deposition of SiC in the pores of the SiC preform was realized by decomposition of methyltrichlorosilane in hydrogen:

$$CH_3SiCl_{3(l)} + (n)H_{2(g)} \rightarrow SiC_{(s)} + 3HCl_{(g)} + H_{2(g)}$$
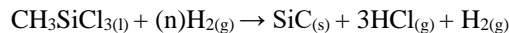
The quartz jar was the reaction vessel that protected the cavity's and waveguide's walls from the corrosive reactants and by-products of the decomposition reaction. The hollow quartz stand was the entry point of the gas and supported the sample which was placed between two alumina foam rings. The photo of the interior of the cavity is shown in Fig. 1(a).

The experiments have successfully demonstrated efficiency of the ME CVI process for production of SiCf/SiC composites. Two densified samples are exemplified in Fig. 2 – the brighter areas are the evidence of substantial amount of SiC deposited. The results showed a clear potential for achieving full density for up to 10 days, and that would translate to a time reduction of 90% in comparison with conventional CVI production of this composite.
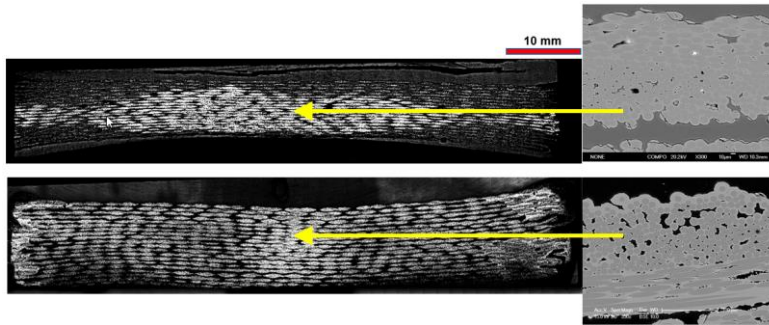
Fig. 2. Optical microscope images of the SiC$_f$/SiC composite densified by the ME CVI
in the SAIREM's Labotron HTE M30KB CL PRO system.

However, the process was difficult to control, and the experimental work suffered from a severe lack of reproducibility. In particular, it was observed that, in some cases, heating rate changed with time while the input power remained constant, and small, supposedly negligible changes in geometry resulted (or did not result) in very different heating processes. Experimental resolution of these issues was difficult because of the hazardous environment (very high temperature, gaseous medium around the processed material). Hence a dedicated computational study was undertaken in order to clarify the causes of the peculiar effects in the experiments and help improve the control over the process.

3. Computer Model

ME CVI is a very complex phenomenon involving multiple interacting physical and chemical processes, but mimicking them all in a unified multiphysics model was not in the scope of this work. Our modelling objective was to single out the interaction of the heated SiC sample with the microwaves and analyse the mechanisms of formation of microwave-induced temperature fields in the experimental system. Simulations were done for the SiC disc of three sizes, *A* (*d* = 55 mm, *h* = 8 mm), *B* (*d* = 110 mm, *h* = 16 mm), and *C* (*d* = 165 mm, *h* = 24 mm), in the SAIREM's Labotron HTE M30KB CL PRO system.

The model was built for the Finite-Difference Time-Domain (FDTD) simulator *QuickWave*^{TM} [12]. Fig. 1(b) shows a 2D view of the model in the software's interface. The procedure for solving the EM-thermal fully coupled problem is similar to the one outlined in [13-16]. The EM and thermal solvers operate as parts of an iterative procedure in which a steady state solution of the EM problem becomes an input for the thermal simulator computing the temperature field induced after a pre-set heating time step. After each iteration, material parameters are upgraded in every cell of the FDTD mesh in accordance with the temperature field outputted from the thermal solver.

Temperature characteristics of EM material parameters, dielectric constant ε' and the loss factor ε'', and of thermal material parameters, specific heat C_p, density δ, and thermal conductivity k, were determined in the entire temperature range ($20 \leq T \leq 1,200$ºC) through dedicated measurements and required post-processing of the measured data. These characteristics are a critical part of input data of the EM-thermal coupled simulation [13-16]. The values of ε' and ε'' of the SiC sample are much higher than the ones of alumina foam and quartz, and both $\varepsilon'(T)$ and $\varepsilon''(T)$ are nonlinear increasing functions of temperature. While density of all the materials was assumed constant in the heating process, the values of C_p and k of all the materials are comparable and nonlinearly increase/decrease, respectively, with temperature. The details on the data on all the material parameters can be found in [7].
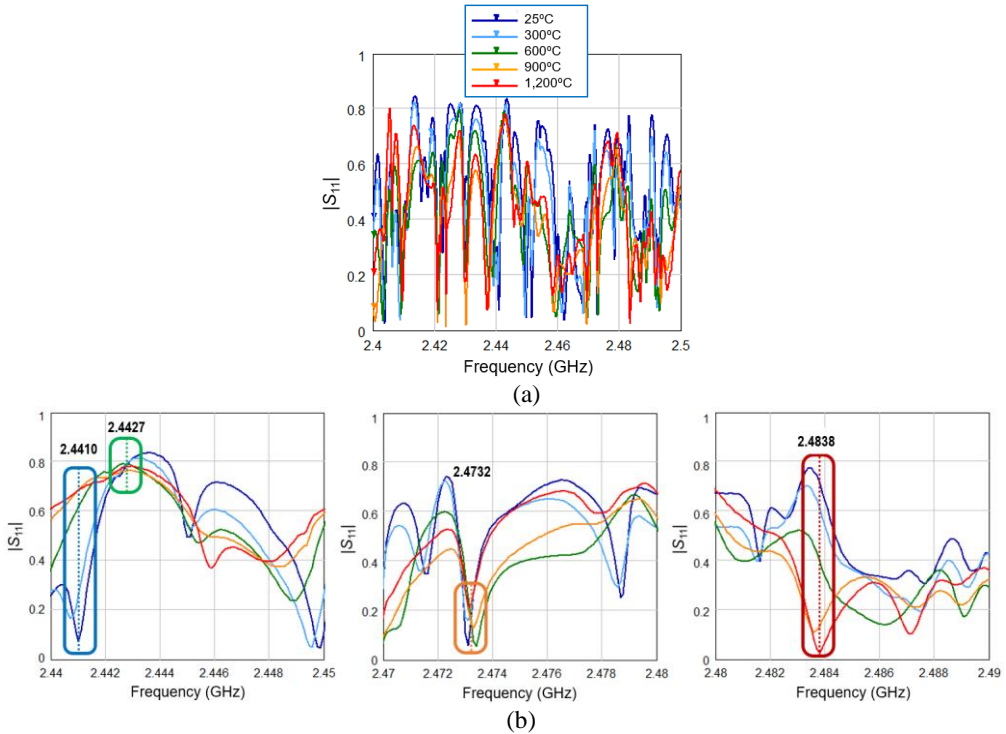
Fig. 3. Frequency characteristics of the reflection coefficient characteristics in the process of heating of disc *B* in the IMS range of 2.45 GHz (a) and in its three subintervals containing frequencies at which $|S_{11}|$ is high (green frame), low (orange frame), increasing (blue frame), and decreasing (red frame) (b).

4. Computational Results

Simulations were performed on a Windows 10 workstation with two Intel Xeon Gold 5120 processors with a base/peak frequency of 2.2/3.2 GHz and the GPU NVIDIA Quadro P5000.

Since the microwave heating rate is conditioned by energy coupling, at the first stage of our modelling effort, the EM part of the model was used to determine frequency characteristics of the reflection coefficient ($|S_{11}|$) of the microwave system. For each disc, these characteristics were obtained for several temperature values spread across the entire temperature range of the heating process. Temperature in the EM problem was represented through corresponding values of ε' and ε''.

Simulated $|S_{11}|(f)$ curves allowed us to see the impact made by the dielectric properties changing while heating on the reflection coefficient (and thus energy coupling). Six typical frequency characteristics are shown in Fig. 3. It turned out that, depending on frequency, $|S_{11}|$ may behave differently with temperature going up: with frequency kept constant, it may remain low, or high, or increase, or decrease. In Fig. 3, these behaviours of $|S_{11}|$ are associated with particular highlighted frequencies. Also, due to the presence of multiple narrow resonances, a large difference in reflection may result from very small frequency changes. The obtained $|S_{11}|(f)$ curves, therefore, provide significant evidence for unpredictable changes in the heating rate in the experiments with constant input power. They are also consistent with the results of [17] concluded, through an applicable sensitivity analysis, that frequency was the most critical factor in stability of MW CVI process.

Table 1. Frequencies Causing Distinct Behaviours of the Reflection Coefficient
in Microwave Heating of Discs *B* and *C*.

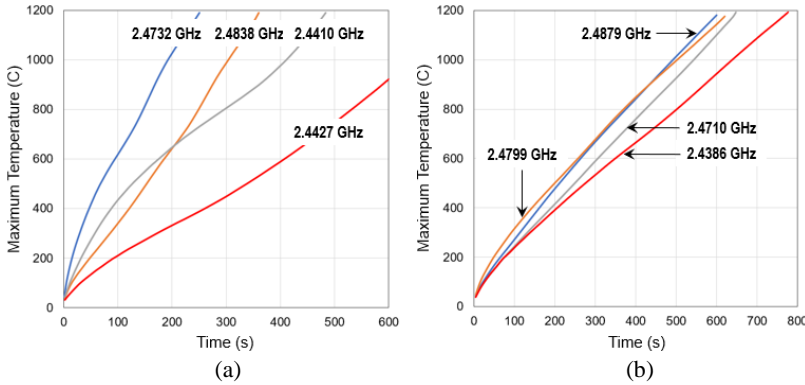| SiC disc: Reflections (coupling):	*B* (d = 110 mm, h = 16 mm)	*C* (d = 165 mm, h = 24 mm)
Increasing $\|S_{11}\|$ (decreasing coupling)	2.4410 GHz	2.4799 GHz
Decreasing $\|S_{11}\|$ (increasing coupling)	2.4838 GHz	2.4710 GHz
$\|S_{11}\|$ constant low (high coupling)	2.4732 GHz	2.4879 GHz
$\|S_{11}\|$ constant high (low coupling)	2.4427 GHz	2.4386 GHz

Fig. 4. Time characteristics of maximum temperature in the heated SiC discs *B* (a) and *C* (b) at
four frequencies associated with different behaviour of the reflection coefficient as in Table 1.

At the next stage, temperature fields induced in the processed SiC sample at the frequencies associated with distinct behaviours of the reflection coefficient (Table 1) were simulated. Strongest difference in the heating rate was observed in case of disc *A* when, at one frequency, maximum temperature of 1,200°C was reached in 130 s, whereas, at another frequency, 300°C was barely achieved after 400 s. Fig. 4 shows the time-temperature characteristics for discs *B* and *C*. It is seen that, for the larger sizes of the material with high losses, the difference in the heating rates is less pronounced. This is explained by the fact that in these cases the average values of $|S_{11}|$ are lower and the $|S_{11}|(f)$ curves are characterised by not so strong and narrow resonances.

The graphs in Fig. 4 are about maximum temperature whose locations in the sample are not specified as they vary in the course of the heating process. Fig. 5 presents typical time evolution of temperature patterns in the horizontal (XY) and vertical (XZ) coordinate planes through the centre of the SiC disc and through the centre of both the disc and the alumina foam holders, respectively. As expected, in the beginning of microwave processing, temperature distributions in the heated sample are highly nonuniform: indeed, the patterns then follow distributions of dissipated EM power which are intrinsically nonuniform and have dissimilar profiles at different frequencies due to distinct structures of the electric field. With heating time going on, however, the patterns become more unform; one of the principal reasons for that is the relatively high thermal conductivity of SiC that supports the spread of heat throughout the sample's volume.

The process of temperature homogenization was also quantitatively analysed with the use of the computational procedure checking the fields against a special metric of temperature field uniformity λ_T [18]. The metric is based on the standard deviations and the means of temperature values in the pattern after every heating time step; the more uniform the
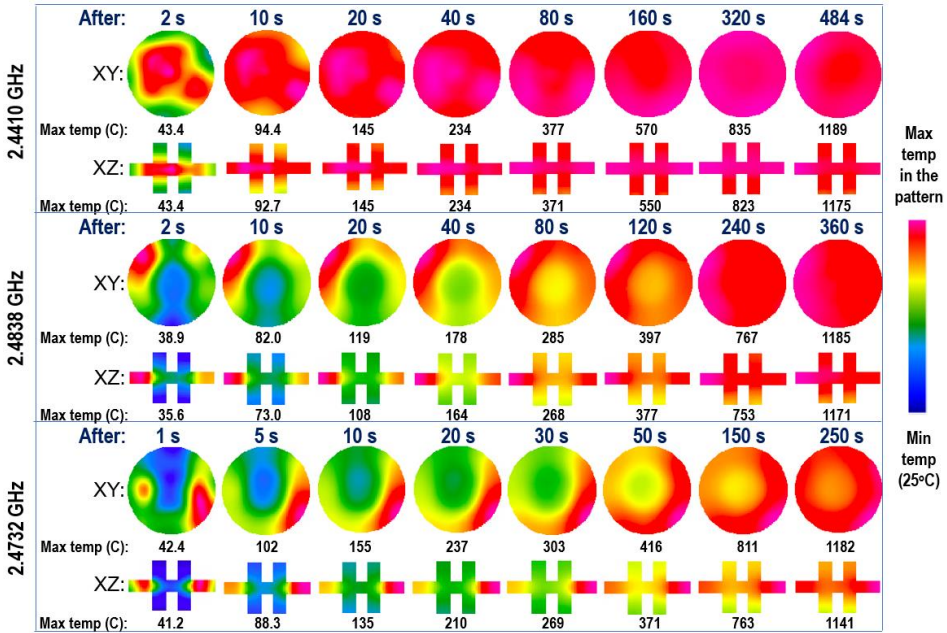
Fig. 5. A series of XY and XZ cross sectional time evolution of temperature patterns in the SiC disc held between the two alumina foam rings during microwave heating at three frequencies characterized in Table 1. Presented time instances are specified on the top of each process; maximum temperature values in each pattern are below their images. Input power 1.1 kW.
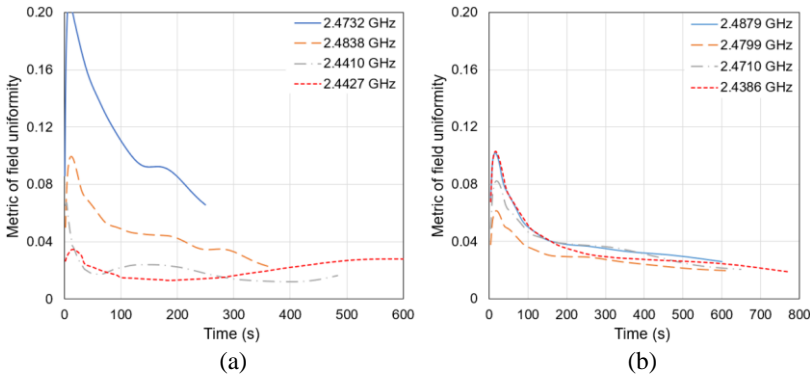

Fig. 6. Time evolution of the metric of uniformity of temperature field induced by the microwaves at different frequencies for discs *B* (a) and *C* (b).

distribution, the smaller the value of λ_T. In Fig. 6, λ_T is plotted against the heating time in the processes with discs *B* and *C*. The decreasing values of the metric confirm what is visually seen in Fig. 5 where the homogenisation of the temperature patterns occurs with increasing time and temperature. The levels of uniformity in the faster and slower processes (at 2.4732 and 2.4410 GHz) in Fig. 5 are consistent with the blue and grey curves in Fig. 6 (a). It is also seen that while the slower processes in the considered SiC samples are caused by weaker energy coupling, they lead to more homogeneous temperature distributions.

4. Conclusion

In this paper, we have presented typical results of the computational study undertaken to clarify the causes of some experimental issues in production of SiC$_f$/SiC composites by ME CVI in the SAIREM's Labotron HTE M30KB CL PRO system. With the use of the FDTD EM model of the scenario, it has been demonstrated that, when processing a small disc of SiC in a large Labotron's cavity, energy coupling may be extremely sensitive to frequency. Since the EM material parameters, dielectric constant ε' and the loss factor ε'', vary with temperature, the coupling may also significantly change in the course of heating even when frequency is fixed.

An FDTD EM-thermal coupled model applied to the same scenario has revealed that patterns of microwave-induced temperature fields are considerably different at different frequencies. Depending on the level of coupling at the given frequency, the heating rate can be high, or low, or it can vary. Simulation of time evolution of temperature fields has revealed that initially non-uniform patterns within the SiC sample gradually even up. With 1.1 kW of input power and a high heating rate, maximum temperature of the process (1,200ºC) can be reached, depending on the size of the SiC disc (*A*, *B*, *C*), for 130 to 600 s. The level of uniformity and energy coupling (or the heating rate) clearly appear as a trade-off: the slower the heating process, the more homogeneous the temperature pattern in the upper end of the temperature range of the process.

The performed computational study also illuminates the well-known observation that the magnetron-based processes of heating of small pieces of absorbing materials in large microwave cavities are naturally hard to control. Smaller applicators fed by solid-state generators give increasing flexibility in choosing (and, if necessary, alternating) frequency of thermal processing, the amplitude of the field, and hence in maintaining desirable heating regimen [19].

Overall, this work has clearly highlighted the need and value of FDTD multiphysics modelling capabilities to support complex experimental studies in microwave power engineering. Without this tool research cannot be proactive in the design of experiments, and it is limited in the understanding afforded by experimental work. In the reported study, the EM and EM-thermal models of the microwave system have provided insight where experiments and measurement tools and equipment cannot do that.

References
1. Giurgiutiu, V., *Structural Health Monitoring of Aerospace Composites*, Academic Press, 2016.
2. Jaglin, D., et al, *J. Amer. Ceramic Soc.*, 2006, **89**, 2710-2717.
3. Binner, J., et al, *Advances in Applied Ceramics,* 2013, **112**, 235-241.
4. Binner, J., et al, *Proc. 54th IMPI's Microwave Power Symp. (Virtual, June 2020)*, pp. 23-25.
5. Timms, L.A., et al, *J. Microsc.*, 2001, **201**, 316-323.
6. Binner, J., et al, *Int. Mater. Rev*., 2020, **65**, 389-444.
7. Porter, M., *High-Temperature Ceramic Matrix Composites Prepared via Microwave Energy Enhanced Chemical Vapour Infiltration*, Ph.D. Dissertation, University of Birmingham, U.K., 2020.
8. D'Ambrosio, R., et al, *Chem. Eng. J.*, 2021, **405**, 126609.
9. Lazzeri, A., In: *Ceramics and Composites Processing Methods*, N.P. Bansal and A. R. Boccaccini, Eds., John Wiley & Sons, 2012.
10. Coltelli, M.-B. and Lazzeri, A., In: *Chemical Vapour Deposition (CVD) – Advances, Technology, and Applications*, K.L. Choyp, Ed., CRC Press, 2019.
11. Tang, S., et al, *J. Mater. Sci. Technol*., 2017, **33**, 117-130.

12. *QuickWave*TM, 1998-2021, QWED Sp. Z.o.o., https://www.qwed.com.pl.
13. Kopyt, P. and M. Celuch, *J. Microwave Power & Electroman. Energy*, 2007, **41**, 18-29.
14. Celuch, M. and P. Kopyt, In: *Development of Packaging and Products for Use in Microwave Ovens*, M. Lorence and P. Pesheck, Eds., Woodhead Publishing, 2009, pp. 305–348.
15. Koutchma, T.V. and V.V. Yakovlev, In: *Mathem. Analysis of Food Processing*, M. Farid, Ed., 2010, pp. 625-657.
16. Yakovlev, V.V., et al, In: *Microwave and RF Power Applications*, J. Tao, Ed., Cépaduès Éditions, 2011, pp. 303-306.
17. Maizza, G. and M. Longhin, *Proc. of the COMSOL Conference (Milan, 2009)*, 7 p.
18. Kumi, P. and V.V. Yakovlev, *Proc. 53rd IMPI's Microwave Power Symp. (Las Vegas, NV, June 2019)*, pp. 123-125.
19. Yakovlev, V.V., *J. Microwave Power & Electromag. Energy*, 2018, **52**, 31-44.